PCCP

Accepted Manuscript

ROYAL SOCIETY OF CHEMISTRY

www.rsc.org/pccp

THEORY OF THE FORMATION OF THE ELECTRIC DOUBLE LAYER AT THE ION EXCHANGE MEMBRANE-SOLUTION INTERFACE

A.A. Moya

Universidad de Jaén, Departamento de Física, Edificio A-3, Campus Universitario de Las Lagunillas - 23071 Jaén, Spain.

Jan 2015

ABSTRACT

This work aims to extend the study on the basis of the Nernst-Planck and Poisson equations of the formation of the electric double layer at the interface defined by a solution and an ion-exchange membrane, including different values for the counter-ion diffusion coefficient and the dielectric constant in the solution and membrane phases. The network simulation method is used to obtain the time evolution of the electric potential, the displacement electric vector, the electric charge density and the ionic concentrations at the interface between a binary electrolyte solution and a cation-exchange membrane with total co-ion exclusion. The numerical results for the temporal evolution of the interfacial electric potential and the surface electric charge are compared with analytical solutions derived in the limit of the shortest times by considering the Poisson equation with a simple cationic diffusion process. The steady-state results are justified from the Gouy-Chapman theory for the diffuse double layer in the limits of similar and high bathing ionic concentration with respect to the fixed-charge concentration inside the membrane. Interesting new physical insights arise from the interpretation of the process of the formation of the electric double layer at the ion exchange membrane-solution interface on the basis of a membrane model with total co-ion exclusion.

Keywords: Electrodiffusion processes / Nernst-Planck and Poisson equations / Electric double layer / Network simulation method / Ion-exchange membranes / Dielectric mismatch

1. INTRODUCTION

The equilibration of spatially heterogeneous liquid systems where ionic species have unequal transport coefficients is a classical research line in the field of physical chemistry. This problem has recently been revised from a theoretical viewpoint by using modern and advanced numerical methods to deal with the mono-dimensional Nernst-Planck and Poisson equations, the main attention being paid to free liquid junctions[1-4] and electrolyte solutions separated by semi-permeable infinitesimal membranes[5-6]. The temporal evolution to the equilibrium steady-state of the electric potential, the surface electric charge, and the profiles of the electric field, electric charge density and ionic concentrations have been analyzed for the different types of free liquid junctions usually found in the literature. The infinitesimal membranes have been chosen because of its significance in biological cells and its fundamental character in biophysics and biochemistry.

Ionic transport processes through ion-exchange synthetic membranes and related ion-selective systems, particularly fluidic devices, are receiving special attention from the scientific community. An ion-exchange membrane is a layer of material with inner electric charge that separates two solutions phases. Conventional membranes present fixed or mobile ionic sites and they are partially permeable or fully impermeable to at least one dissolved ionic component. An ion-exchange membrane is ideal when the fluxes of the co-ions are zero, i.e., it presents total co-ion exclusion. Such membranes find a wide range of application in physics and chemistry, particularly in the field of brackish water or seawater desalination[7] and in that of ion-selective electrodes used as chemical sensors,[8] although there is a growing interest in the field of renewable energies such as pressure-retarded

osmosis and reverse electrodialysis[9] as well as in their use as separators in fuel cells,[10] redox flux batteries,[11] or joined to porous electrodes in energy production by expansion of electrical double layers[12] or desalination by capacitive deionization.[13] The study of the equilibration of the solutions inner and outer in an ion-exchange membrane system is interesting not only from the fundamental viewpoint but also from the practical viewpoint because it can find application, for example, into the characterization of the time of response and the temporal evolution to the equilibrium steady-state of ion-selective electrodes in chemical sensoring, electrode-membrane assemblies in renewable energy harvesting, or micro-nanochannel interfaces in fluidic devices. Apart from the existence of fixed-charge in one of the phases, the main novelty with respect the above cited systems, such as liquid junctions and infinitesimal membranes, is the consideration of different values for the ionic diffusion coefficients and the dielectric constant in the solution and membrane phases, these aspects being of a major interest in ion-exchange systems. The consideration of different values of the diffusion coefficient of the counter-ion in the membrane and the solutions phases is usual in the study of the response of ion-exchange membrane systems to external electrical perturbations and it is a consequence of the experimental values measured for the resistance or conductance of the membrane.[14-15] In addition, decreasing in dielectric constant of a solution with an increasing electrolyte concentration is a well-known fact[16-17] and the dielectric mismatch is included in the modern theoretical formulations on ionic transport in ion-exchange membrane systems.[18] Particularly, the dielectric mismatch in ion-exchange membrane systems has been previously incorporated in studies dealing with ionic transport including ion-solvent interactions[19] and with the equilibrium electric potential in systems with multi-ionic electrolytes.[20-22] Also, there is a number of studies dealing with the

electrochemical properties of specific membranes with low electric permittivity,[23] particularly interesting being those in the field of ion-selective electrodes.[24,25] However, to our knowledge, fixed-charge concentration in one of the phases, and different values for the counter-ion diffusion coefficient and the dielectric constant in the membrane and solution phases are topics which have not been previously dealt with in the literature in the framework of the transient equilibration of electrolytic solutions.

This work aims to extend the study of the formation of the electric double layer at the interface defined by a solution and an ion-exchange membrane, including different values for the counter-ion diffusion coefficient and the dielectric constant in the solution and membrane phases. On the basis of interesting previous numerical treatments in this field,[26-31] the ionic transport processes are described by the Nernst-Planck and Poisson equations in both the membrane and the diffusion boundary layer in the binary electrolyte solution adjacent to the membrane. It is well-known that the ionic concentrations in the bulk of the membrane depend on the bathing salt concentration because of the ionic partitioning. For the sake of simplicity and greater generality, we have chosen a membrane with total co-ion exclusion and thus the initial counter-ion concentration inside the membrane is constant and equal to the equivalent fixed-charge concentration. The boundary conditions for the Nernst-Planck flux equations are the constant ionic concentrations in the bathing solution, the constant counter-ion concentration inside the membrane, the zero value of the co-ion flux at the outer boundary of the membrane and the continuity of the counter-ion flux at the interface. For the Poisson equation, the origin of the electric potential, the continuity of the electric displacement vector at the interface, and the fact that the electric current must to be zero in equilibrium systems, are used as the boundary conditions. In this paper, the network

simulation method[32] is used as an appropriate and powerful numerical tool based on a finite differences scheme to simulate the formation of the electric double layer at the interface between a binary electrolyte solution and a cation-exchange membrane with total co-ion exclusion.

The numerical results for the temporal evolution of the interfacial electric potential and the surface electric charge are compared with analytical solutions derived in the limit of the shortest times by considering a simplified model based on the Poisson equation with a simple cationic diffusion process. The steady-state results are justified from the Gouy-Chapman theory for the diffuse double layer in the limits of similar and high bathing ionic concentration with respect to the fixed-charge concentration inside the membrane. Interesting new physical insights arise from the interpretation of the process of the formation of the electric double layer at the ion exchange membrane-solution interface on the basis of a membrane model with total co-ion exclusion.

2. IONIC TRANSPORT PROCESSES IN ION-EXCHANGE MEMBRANE SYSTEMS

We will consider the interface defined by an ion-exchange membrane and a diffusion boundary layer adjacent to the membrane. The membrane is supposed to completely block the transport of anions. If the ionic transport is one-dimensional, in the x direction, and perpendicular to the membrane-solution interface at x=0, the equations in dimensionless form (see Appendix A) determining the behaviour of the binary electrolyte in the diffusion boundary layer, extended from x=-L to x=0, i.e., for x<0, at time t are the laws of mass

conservation or continuity equations:

$$\frac{\partial J_i(x,t)}{\partial x} = -\frac{\partial c_i(x,t)}{\partial t}, \qquad i = 1, 2 \tag{1}$$

the Nernst-Planck flux equations written for dilute solutions:

$$J_i(x,t) = -D_{iS}\left[\frac{\partial c_i(x,t)}{\partial x} + z_i\, c_i(x,t)\frac{\partial \phi(x,t)}{\partial x}\right] \tag{2}$$

and the Poisson equation:

$$\frac{\partial \boldsymbol{D}(x,t)}{\partial x} = \sum_i z_i\, c_i(x,t) = \rho(x,t) \tag{3}$$

where

$$\boldsymbol{D}(x,t) = -\varepsilon_S \frac{\partial \phi(x,t)}{\partial x} = -\varepsilon_S\, E(x,t) \tag{4}$$

Here $J_i(x,t)$, D_{iS}, $c_i(x,t)$ and z_i denote the ionic flux, the diffusion coefficient in the solution, the molar concentration and the charge number of ion i, respectively. The electric potential is represented by $\phi(x,t)$, the electric permittivity in the solution phase by ε_S, the electric displacement vector by $\boldsymbol{D}(x,t)$, the electric charge density by $\rho(x,t)$, and the electric field by $E(x,t)$. The constants F, R and T have their usual meanings: Faraday constant, ideal gas constant and absolute temperature, respectively.

Now, the behaviour of the counter-ion inside the interfacial region of the membrane, extended from x=0 to x=L, i.e., for x>0, at time t is described by the law of mass conservation or continuity equation:

$$\frac{\partial J_1(x,t)}{\partial x} = -\frac{\partial c_1(x,t)}{\partial t} \tag{5}$$

the Nernst-Planck flux equation written for dilute solutions:

$$J_1(x,t) = -D_{1M}\left[\frac{\partial c_1(x,t)}{\partial x} + z_1 c_1(x,t)\frac{\partial \phi(x,t)}{\partial x}\right] \quad (6)$$

where D_{IM} is the diffusion coefficient in the membrane phase, and the Poisson equation:

$$\frac{\partial \boldsymbol{D}(x,t)}{\partial x} = z_1 c_1(x,t) - X = \rho(x,t) \quad (7)$$

where

$$\boldsymbol{D}(x,t) = -\varepsilon_M \frac{\partial \phi(x,t)}{\partial x} = -\varepsilon_M E(x,t) \quad (8)$$

respectively being X and ε_M, the fixed-charge concentration and the dielectric permittivity inside the membrane. It is worth noting that we have considered an ideal fixed-charge membrane and the transport of the co-ion is supposed to be negligible inside the membrane. This is a usual experimental situation because the counter-ion transport number is usually close to unity, which allows us to obtain the diffusion coefficient of the counter-ion from the measure of the resistance or conductance of the membrane.[33] This hypothesis allows us to simplify the computation problem by ignoring the ionic partitioning at the interface and so by doing negligible the changes in the cationic concentration inside the membrane with the bathing salt concentration, which could make difficult the choice of the initial conditions of the system. In addition, it must be mentioned that the total co-ion exclusion hypothesis is widely used in the framework of the space charge model, which considers the membrane as composed of an array of identical parallel charged cylindrical pores, because it leads to a steady-state analytical solution for the Poisson-Boltzmann equation.[18] In connection with this later, it is so desirable to generalize the study of the formation of the electric double

layer on the basis of the Nernst-Planck and Poisson equations to multiple dimensions, according to the previous studies in mixed conductors used in fuel cells,[34,35] because it find application in nanoporous membranes or in related fluidic micro and nanochannels.

On the other hand, the total electric current through the system, $I(x,t)$, is the sum of the faradaic and displacement currents:

$$I(x,t) = \sum_i z_i J_i(x,t) + \frac{\partial \boldsymbol{D}(x,t)}{\partial t} \quad (9a)$$

and from eqs. 1-4 for the solution phase or from eqs. 5-8 for the membrane phase, one obtains:[27,28]

$$\frac{\partial I(x,t)}{\partial t} = 0 \quad (9b)$$

i.e., it is not a function of the position, $I(x,t)=I(t)$. Therefore, the electric current can be evaluated at an arbitrary point of the system such as $x=-L$.

If we consider a binary electrolyte with the cationic concentration c^0 at the bulk of bathing solution, the Dirichlet-type outer boundary conditions for the flux equations are:

$$c_1(-L,t) = c^0 \quad (10a)$$

$$c_2(-L,t) = -\frac{z_1}{z_2} c^0 \quad (10b)$$

$$c_1(L,t) = \frac{X}{z_1} \quad (10c)$$

while at the interface, at $x=0$, it must be imposed the continuity of the fluxes of the permeant ionic species:

$$J_1(0^-,t) = J_1(0^+,t) \quad (11a)$$

and the zero value of the fluxes of the impermeant ionic species:

$$J_2(0,t) = 0 \tag{11b}$$

Now, if one considers the equilibrium state of the system, I=0, the outer boundary conditions for the Poisson equation can be expressed as:[27,28]

$$\frac{d\,\boldsymbol{D}(-L,t)}{d\,t} = -\sum_i z_i J_i(-L,t) \tag{12a}$$

$$\phi(L,t) = 0 \tag{12b}$$

Equation 12a is a Neumann-type boundary condition for the Poisson equation and it is obtained from eq. 9a for I=0. Equation 12b is the usual Dirichlet-type boundary condition for the Poisson equation defining the reference level for the electric potential at x=L inside the membrane. Now, at the interface, at x=0, it must be imposed the continuity of the electric displacement vector:

$$\boldsymbol{D}(0^-,t) = \boldsymbol{D}(0^+,t) \tag{13}$$

It must be noted that we impose the continuity of the electric displacement vector instead of the electric field, as it has been done in other previous papers,[5,6] because we intend to include the dielectric mismatch between the solution and membrane phases.

On the other hand, an initial state must be specified in order to study the time evolution of the system. The initial conditions for the ionic concentrations in the diffusion boundary layer, from x=-L to x=0^-, are:

$$c_1(x,t=0) = c^0 \tag{14a}$$

$$c_2(x,t=0) = -\frac{z_1}{z_2}c^0 \tag{14b}$$

and the initial condition for the counter-ion concentration inside the membrane is:

$$c_1(x,t=0) = \frac{X}{z_1} \quad (14c)$$

while the initial condition for the electric potential in the complete system, from x=-L to x=L, is:

$$\phi(x,t=0) = 0 \quad (14d)$$

Finally, the surface electric charge in the diffuse layer corresponding to the solution phase, σ, is:

$$\sigma(t) = \int_{-L}^{0} \rho(x,t)\,dx = \boldsymbol{D}(0,t) - \boldsymbol{D}(-L,t) \quad (15a)$$

while that in the membrane phase, σ_M, is:

$$\sigma_M(t) = \int_{0}^{L} \rho(x,t)\,dx = \boldsymbol{D}(L,t) - \boldsymbol{D}(0,t) \quad (15b)$$

Now, if we chose the length L in such a way that when the equilibrium steady-state of the system is reached, the electric displacement vectors at the boundaries of the system are zero:

$$\boldsymbol{D}(-L,t) = \boldsymbol{D}(L,t) = 0 \quad (16a)$$

one obtains the following relation:

$$\sigma_M(t) = -\boldsymbol{D}(0,t) = -\sigma(t) \quad (16b)$$

3. DYNAMICS OF THE INTERFACIAL ELECTRIC POTENTIAL AT THE SHORTEST TIMES

At the shortest times, the membrane system potential, $\phi_M(t)$=ϕ(-L,t), and the surface

electric charge density in the diffuse double layer at the solution, $\sigma(t)$, can be theoretically estimated by considering the ionic transport controlled by semi-infinite diffusion processes.[36] Since the linear diffusion partial differential equation in the solution phase (x<0) is:

$$\frac{\partial c_1(x,t)}{\partial t} = D_{1S}\frac{\partial^2 c_1(x,t)}{\partial x^2} \quad (17a)$$

and that in the membrane phase (x>0) phase is:

$$\frac{\partial c_1(x,t)}{\partial t} = D_{1M}\frac{\partial^2 c_1(x,t)}{\partial x^2} \quad (17b)$$

by taking the Laplace transform, one obtains:

$$S\overline{c_1} - c^0 = D_{1S}\frac{d^2\overline{c_1}}{dx^2} \quad (18a)$$

$$S\overline{c_1} - \frac{X}{z_1} = D_{1M}\frac{d^2\overline{c}}{dx^2} \quad (18b)$$

These equations must be solved hold to the following boundary conditions:

$$\overline{c_1}(x\to-\infty) = \frac{c^0}{S} \quad (19a)$$

$$\overline{c_1}(x\to\infty) = \frac{X}{z_1 S} \quad (19b)$$

$$\overline{c_1}(x=0^-) = \overline{c_1}(x=0^+) \quad (19c)$$

$$D_{1S}\left.\frac{d\overline{c_1}}{dx}\right|_{x=0^-} = D_{1M}\left.\frac{d\overline{c_1}}{dx}\right|_{x=0^+} \quad (19d)$$

In this way, one obtains the following equation in the solution phase (x<0):

$$\overline{c_1} = \frac{\frac{X}{z_1} - c^0}{\alpha S} \exp\left(x\sqrt{\frac{S}{D_{1S}}}\right) + \frac{c^0}{S} \tag{20a}$$

and the following other in the membrane phase (x>0):

$$\overline{c_1} = (1-\alpha)\frac{\frac{X}{z_1} - c^0}{\alpha S} \exp\left(-x\sqrt{\frac{S}{D_{1M}}}\right) + \frac{X}{z_1 S} \tag{20b}$$

where:

$$\alpha = \frac{\sqrt{D_{1S}} + \sqrt{D_{1M}}}{\sqrt{D_{1M}}} \tag{21}$$

Now, the Laplace transform of the electric charge density can be written in the solution phase as:

$$\overline{\rho} = z_1\left(\overline{c_1} - \frac{c^0}{S}\right) = \frac{X - z_1 c^0}{\alpha S} \exp\left(x\sqrt{\frac{S}{D_{1S}}}\right) \tag{22a}$$

and that in the membrane phase is:

$$\overline{\rho} = z_1\overline{c_1} - \frac{X}{S} = (1-\alpha)\frac{X - z_1 c^0}{\alpha S} \exp\left(-x\sqrt{\frac{S}{D_{1M}}}\right) \tag{22b}$$

In this way, the Laplace transform of the electric displacement vector in the solution phase is:

$$\overline{\boldsymbol{D}} = \int_{-\infty}^{x} \overline{\rho}\, dx = \frac{X - z_1 c^0}{\alpha S}\sqrt{\frac{D_{1S}}{S}} \exp\left(x\sqrt{\frac{S}{D_{1S}}}\right) \tag{23a}$$

and that in the membrane phase is:

$$\overline{\boldsymbol{D}} \;=\; -\int_x^{\infty} \overline{\rho}\, dx \;=\; \frac{X - z_1 c^0}{\alpha S}\sqrt{\frac{D_{1S}}{S}}\exp\left(-x\sqrt{\frac{S}{D_{1M}}}\right) \tag{23a}$$

and the Laplace transform of the surface charge density can be written as:

$$\overline{\sigma} \;=\; \overline{\boldsymbol{D}}(x=0) \;=\; \frac{1}{2}\gamma\frac{X - z_1 c^0}{S^{3/2}} \tag{24}$$

where:

$$\gamma \;=\; \frac{2\sqrt{D_{1S}\; D_{1M}}}{\sqrt{D_{1S}} + \sqrt{D_{1M}}} \tag{25}$$

Finally, by considering the Poisson equation, the Laplace transform of the electric potential of the system is:

$$\overline{\phi_S} \;=\; \int_{-\infty}^{0} \frac{\overline{\rho}}{\varepsilon_S}\, dx + \int_0^{\infty} \frac{\overline{\rho}}{\varepsilon_M}\, dx \;=\; \frac{1}{2}\gamma\,\frac{X - z_1 c^0}{S^2}\left(\frac{\sqrt{D_{1S}}}{\varepsilon_S} + \frac{\sqrt{D_{1M}}}{\varepsilon_M}\right) \tag{26}$$

In this way, the inverse Laplace transform can be taken in the above expressions, and the surface charge density is given by:

$$\sigma\,(t) \;=\; \gamma\,(X - z_1 c^0)\sqrt{\frac{t}{\pi}} \tag{27}$$

while the system potential is given by:

$$\phi_M\,(t) \;=\; \frac{\gamma}{2}\left(X - z_1 c^0\right)\left(\frac{\sqrt{D_{1S}}}{\varepsilon_S} + \frac{\sqrt{D_{1M}}}{\varepsilon_M}\right) t \tag{28}$$

Now, it must be highlighted that for $D_{1S}=D_{1M}$ and $\varepsilon_M=\varepsilon_S$, the above expressions are in good agreement with those previously derived in liquid junctions and systems with infinitesimal membranes.[5]

4. RESULTS AND DISCUSSION

In this paper, the results are numerically obtained by using the network simulation method,[32] which is briefly described in Appendix B. A uni-univalent binary electrolyte, z_1=1 and z_2=-1, in systems with L=20, ε_S=4, D_{1S}=1, D_{2S}=1.5, X=5, and different values of D_{1M}, ε_M, and c^0, has been considered. These values could correspond to a sodium chloride solution, and they are very similar to those used in previous papers, which deal with the electrochemical impedance of ion-exchange membrane systems.[37-39] We have chosen a 1:1 binary electrolyte for the sake of simplicity, but we use a membrane with total co-ion exclusion and the obtained results must be qualitatively valid in systems with asymmetric electrolytes.

First of all, it must be noted that the values of the bathing salt concentration, c^0, are smaller than that of the fixed-charge concentration inside the membrane, X. Then, during the process of formation of the electric double layer at the interface, the electric charge density in the solution diffuse layer is positive and it arises from the accumulation of cations at the interfacial region. Conversely, the electric charge in the membrane diffuse layer is negative and it is due to the depletion of counter-ions at the interface. In this way, the electric potential is positive at any time. Moreover, according to the Gouy-Chapman theory for the electric double layer,[36] the steady-state surface electric charge in the solution phase must be independent of the diffusion coefficients but it must be a function of the dielectric permittivity. However, the steady-state system electric potential obeys the Donnan equation and it must be independent of the values of the dielectric constants and the diffusion coefficients.

Figures 1 and 2 respectively show the time evolution of the interfacial electric potential, $\phi_M(t)=\phi(-L,t)$, and the surface electric charge in the solution diffuse layer, $\sigma(t)$ in a system with ε_M=4, c^0=0.5, and different values of the diffusion coefficient of the cation in the membrane, namely, D_{1M}=1, 0.1, and 0.01. In these figures, it is observed that both the membrane potential and the surface charge density transitorily increase from the zero initial value to reach a steady-state value. Since the surface charge density corresponds to the value of the electric displacement vector at the position of the interface at x=0 (Eq. 16b), it represents the maximum value of the electric displacement vector along the system. In Figures 1 and 2, the approximate analytical expressions at short times for the interfacial potential given by eq. 28 and the surface charge density given by eq. 27 have also been represented by means of dotted lines and they are in excellent agreement with the numerical results. In these figures, it can be seen that the steady-state values of the electric potential and the surface electric charge are not a function of the diffusion coefficients, in accord with the Gouy-Chapman theory for the electric double layer. However, in the cited figures it is clearly observed that the time that it is needed to reach the steady-state value increases as the cation diffusion coefficient in the membrane, D_{1M}, decreases.

Figures 3 and 4 respectively show the time evolution of the interfacial potential, $\phi_M(t)=\phi(-L,t)$, and the surface electric charge density in the diffuse double layers, $\sigma(t)$, in systems with D_{1M}=0.1, c^0=0.5, and different values of ε_M, namely, ε_M=4, 2, and 1. These values of ε_M respectively correspond to relative dielectric constants in the membrane of values 80, 40 and 20. In these figures, the approximate analytical expressions at short times for the membrane potential and the surface charge density have also been represented and they are in excellent agreement with the numerical results. In Figure 3 it is observed that the

electric potential increases from the zero initial value to the steady-state value, which is not a function of the electric permittivity. However, in Figure 4 it can be seen that the surface charge density increase from the zero initial value to a steady-state value, which increases as ε_M decreases. Moreover, in this figures, it is observed that the time that is needed to reach the steady-state values is almost independent of the values of the dielectric constants.

Figure 5 shows the steady-state values of the interfacial potential, $\phi_{SS}=\phi(x=-L,t\to\infty)$, and the electric potential difference at the right diffuse double layer, $\phi_R=\phi(x=0,t\to\infty)$, in a system with $D_{1M}=0.1$ and different values of ε_M, namely, $\varepsilon_M=4$, 2 and 1, as a function of the bathing electrolyte concentration, c^0. In a similar way, Figure 6 shows the steady-state value of the surface charge density, $\sigma_{SS}=\sigma(x=0,t\to\infty)$, as a function of the bathing electrolyte concentration, c^0.

The numerical results obtained for the steady-state value of the system electric potential exactly agree with those obtained from the Donnan equilibrium relation:

$$\phi_{SS} = \frac{1}{z_1}\ln\left(\frac{X}{z_1 c^0}\right) \tag{29}$$

and so it is not a function of the dielectric constant. The obtained results for the surface electric charge density and the electric potential can be interpreted from the Gouy-Chapman theory for the electrical double layer. If we denote by ϕ_L the electric potential difference at the diffuse double layer in the solution phase, the following relation is obeyed:

$$\phi_{SS} = \phi_L + \phi_R \tag{30}$$

the surface charge density at the left interface can be written as:

$$\sigma^2 = 2 c^0 \varepsilon_S \left[\frac{X}{z_1 c^0} \exp\left(-z_1 \phi_R\right) - \frac{z_1}{z_2} \left(\frac{X}{z_1 c^0} \right)^{\frac{z_2}{z_1}} \exp\left(-z_1 \phi_R\right) - 1 + \frac{z_1}{z_2} \right] \quad (31a)$$

while that at the right interface is:

$$\sigma_M^2 = 2 X \varepsilon_M \left(\frac{1}{z_1} \exp\left(-z_1 \phi_R\right) - \frac{1}{z_1} + \phi_R \right) \quad (31b)$$

Now, since the absolute value of the surface charge densities must be identical at the two diffuse double layers, by equating the two above expressions, it is possible to numerically find the values of ϕ_R, and next to find the values of σ by substituting into one of the above equations. Table 1 shows the values of ϕ_{SS} obtained from eq. 29 and the numerical results obtained for ϕ_R and σ, by using the software Mathematica®, in systems with z_1=1, z_2=-1, ε_S=4, X=5, and different values of ε_M, and c^0. The results obtained from our simulations are then in excellent agreement with the predicted results in accord with this theory.

In Figure 5, it can be seen at the left of the plot that the slope of the electric potential difference at the right diffuse double layer increases as the electric permittivity of the membrane decreases for the highest values of c^0. This behaviour can be justified by considering the Debye-Hückel approximation to the Gouy-Chapman theory, which can be considered valid for the smallest values of the interfacial potential differences (ϕ_L<<1 and ϕ_R<<1) and thus for ionic concentrations close to the fixed-charge of the membrane,[18] $c_0 \approx (X/z_1)$. In such case, the surface charge density in the solution phase can be expressed as:

$$\sigma_{HC} = \phi_L \sqrt{z_1 (z_1 - z_2) c^0 \varepsilon_S} \quad (32a)$$

while that in the membrane phase is:

$$\sigma_{MHC} = -\phi_R \sqrt{z_1 X \varepsilon_M} \quad (32b)$$

In this way, by equating the absolute value of the two above expressions and taking into account eq. 30, it follows:

$$\phi_R = \frac{\phi_{SS}}{1+\sqrt{\frac{X \varepsilon_M}{(z_1-z_2)c^0 \varepsilon_S}}} \quad (32c)$$

in accord with the results previously obtained by Manzanares et al.[40] Here, it can be deduced that, for a given cationic concentration, a decreasing in ε_M leads to an increasing in the interfacial potential ϕ_R, as it is observed in Fig. 5. Now, the surface electric charge is:

$$\sigma_{HC} = \frac{\phi_{SS}\sqrt{z_1(z_1-z_2)c^0 \varepsilon_S}}{1+\sqrt{\frac{(z_1-z_2)c^0 \varepsilon_S}{X \varepsilon_M}}} \quad (32d)$$

and a decreasing in ε_M leads to an increasing in the denominator of this expression and then to a decreasing in the surface electric charge, as it is also observed in Figure 6.

On the other hand, in Figures 5 and 6 it can be appreciated that neither the potential difference at the membrane phase nor the surface electric charge are a function of the ionic concentrations for the highest values of the ionic concentrations occurring at the right of the plots, this situation corresponding to a highly charged membrane. Now, if we consider $c^0 << (X/z_1)$, equation 31a leads to:

$$\sigma_{LC}^2 = 2\frac{\varepsilon_S X}{z_1}\exp\left(-z_1 \phi_R\right) \quad (33a)$$

and by equalling to eq. 31b one obtains the following relation:

$$\frac{1}{z_1}\varepsilon_S \exp\left(-z_1\phi_R\right) = \varepsilon_M\left[\frac{1}{z_1}\exp\left(-z_1\phi_R\right)-\frac{1}{z_1}+\phi_R\right] \quad (33b)$$

and so:

$$\frac{\varepsilon_S-\varepsilon_M}{\varepsilon_M}e^{-z_1\phi_R} = z_1\phi_R - 1 \quad (33c)$$

In these equations the bathing cationic concentration, c^0, does not appear, and it presents analytical solution in terms of the Lambert W-function, which is named *ProductLog*[41] in Mathemathica®:

$$\phi_R = \frac{1}{z_1}\left[1+W\left(\frac{\varepsilon_S-\varepsilon_M}{\varepsilon_M e}\right)\right] \quad (33d)$$

In this way, since $W(0)=0$ and $W(1/e)=0.2785$ and $W(3/e)=0.6035$, we numerically obtain $\phi_R=1$ for $\varepsilon_M=4$, $\phi_R=1.28$ for $\varepsilon_M=2$, and $\phi_R=1.60$ for $\varepsilon_M=1$. Then, it follows $\sigma_{LC}=3.84$ for $\varepsilon_M=4$, 3.34 for $\varepsilon_M=2$, and 2.84 for $\varepsilon_M=1$. The numerical results obtained from our simulations and shown in Figs. 5 and 6 are in excellent agreement with these theoretical results.

On the other hand, Figures 7-11, respectively, exhibit the profiles of the cationic concentration, anionic concentration, electric charge density, electric displacement, and electric potential at the interface of a system with $c^0=0.5$, $D_{1M}=0.1$, $\varepsilon_M=2$, and different times, namely, $t=0.1$, 1, 10 and ∞. For each variable, the profiles are fully asymmetric with respect to the interface at any time because of the different values of the initial concentrations, diffusion coefficients and dielectric constant in the solution and membrane phases.

Figure 7 shows the profile of the counter-ion concentration at the interface at times $t=0.1$, 1, 10 and ∞. In this figure, it can be seen that the initial uniform cationic

concentration in the regions close to the interface increases in the solution and it decreases in the membrane with respect to the equilibrium profiles. The total gradient of the cationic concentration is greater in the membrane phase than in the solution phase at any time. The value of the cationic concentration at the interface at x=0 at the initial instant, $c_1^+ = c_1(x=0,t=0^+)$, can be obtained from eqs. 20a or 20b:

$$c_1^+ = \frac{X - c^0}{\alpha} - c^0 \tag{34a}$$

while the steady-state value, $c_{1SS}=c_1(x=0,t=\rightarrow\infty)$, can be obtained by using the Boltzmann equation[42] with the data in Table 1:

$$c_{1SS} = X \exp\left(-z_1 \phi_R\right) \tag{34b}$$

Then, in our system one obtains c_1^+=1.581 and c_{1SS}=1.808, this small difference being appreciable in Fig. 7. In the steady-state of the system, the cationic concentration profile is uniform and equal to the initial profile approximately for x<-8 in the solution and for x>4 in the membrane. Moreover, in Fig. 7 it is appreciated that the values of the cationic concentrations at t=10 are higher than those at the steady-state in the solution region close to the interface. This behaviour has not been observed in the membrane phase and it can be easily explained as follows. Once the contact has been established at t=0 between the membrane and the solution, the counter-ions diffuse from the membrane to the solution at the interfacial region due to the difference in concentration. Then, an excess of positive electric charge with respect to the initial state appears at the solution diffuse layer and thus an electric field is generated at the interface. This electric field moves the co-ions from the interface to the bulk solution because the membrane is fully impermeable to this kind of

ions, and it causes not only a depletion of co-ions at the interfacial region of the solution but also a weakening of that electric field.

Figure 8 shows the profile of the co-ion concentration at the solution diffuse layer at times t=0.1, 1, 10 and ∞. This profile is nearly uniform throughout the solution at the shortest times. Thus, these results confirm that the ionic transport is controlled by the diffusion of the counter-ion at the shortest times after to establish the contact between the solution and the membrane. As time increases, the values of the co-ion concentration decrease in the region close at the interface with respect to the initial values. In the steady-state of the system, the co-ion maintains the initial uniform profile in the region x<-8. However, it is observed in Fig. 8 that the values of the co-ion concentration at intermediate times are higher than those in the initial state in a small region that is moving away from the interface as time increases. This behaviour is due to the membrane completely blocks the pass of co-ions and this kind of ions moves into the solution bulk, as it has been explained above. The value of the anionic concentration at the inner boundary of the solution at the initial instant is c^0, while the steady-state value, $c_{2SS}=c_2(x=0,t=\rightarrow\infty)$, can be obtained by using the Boltzmann equation[42] with the data in Table 1:

$$c_{2SS} = c^0 \exp\left(z_2 \phi_L\right) \tag{35}$$

Since from Table 1 it follows of ϕ_L=1.286 in our system one obtains c_{2SS}=0.138, which is in excellent agreement with the numerical results.

Figure 9 shows the profiles of the electric charge density at the interfacial region at times t=0.1, 1, 10 and ∞. This figure illustrates the time evolution of the structure of the electric double layer at the solution-membrane interface. The membrane diffuse layer is thinner than the solution one at any time because of the different values of the electric

permittivity. In contrast, the absolute value of the electric charge density at the interface is higher in the membrane diffuse layer than in the solution one. In this figure, it can be seen that the electric charge density profile monotonously expands over time, despite of the anomalous behaviour of the ionic concentrations. In the steady-state, the system keeps electrical neutrality for x<-8 in the solution and for x>4 in the membrane. At the initial instant, the value of the charge density at the inner boundary of the solution can be obtained from eq. 22a and it gives:

$$\rho_S^+ = \frac{X - z_1 c^0}{\alpha} = z_1 c_1^+ + z_2 c^0 \tag{36a}$$

while that at the steady-state is:

$$\rho_{SS} = z_1 c^0 \exp\left(-z_1 \phi_L\right) + z_2 c^0 \exp\left(z_2 \phi_L\right) = z_1 c_{1SS} + z_2 c_{2SS} \tag{36b}$$

and in our system it follows ρ_S^+=1.081 and ρ_{SS}=1.671. The electric charge density at the inner boundary of the membrane is obtained from eq. 22b and it gives:

$$\rho_M^+ = (1-\alpha)\frac{X - z_1 c^0}{\alpha} \tag{37a}$$

while that at the steady-state is:

$$\rho_{MS} = X \exp\left(-z_1 \phi_R\right) - X \tag{37b}$$

and in our system one obtains ρ_M^+=-3.419 and ρ_{MS}=-3.192. All these results related with the electric charge density are in excellent agreement with the numerical results. It is worth noting that in the limit of low salt concentration with respect the membrane fixed-charge concentration, eq. 33d allows us to easily obtain the steady-state value of the electric potential at the interface and thus those of the ionic concentrations and the electric

charge density by using the Boltzmann equation.

Figures 10 and 11 respectively show the profiles of the electric displacement vector and the electric potential at times t=0.1, 1, 10 and ∞. In the steady-state of the system, the maximum value of the electric displacement at x=0 and the value of the membrane potential at x=-L agree with those shown in Table 1. These figures show typical profiles for the displacement electric and the electric potential in free liquid junctions. In accord with the Poisson equation, the slopes of the electric displacement in the solution and membrane phases have the same sign at any time: positive in the solution and negative in the membrane. In the steady-state, the electric displacement is zero and the electric potential constant for x<-8 in the solution and for x>4 in the membrane. As a characteristic behaviour in ion-exchange membrane systems, the electric potential experiences dramatic changes with the time in comparison with those of the ionic concentrations and the electric charge density.

5. CONCLUSIONS

An original study on the basis of the Nernst-Planck and Poisson equations of the formation of the electric double layer at the interface defined by a binary electrolyte solution and an ion-exchange membrane with total co-ion exclusion, including different values of the counter-ion diffusion coefficient and the dielectric constant in the solution and membrane phases, has been presented.

The role played by the counter-ion diffusion coefficient and the dielectric constant in an ion-exchange membrane on the time evolution at the shortest times of the interfacial

electric potential and the surface electric charge, as well as and the transition to the steady-state, has been established during the process of the formation of the electric double layer. It has been obtained that the temporal evolution of the interfacial electric potential and the surface electric charge at the shortest times can be appropriately described by the analytical expressions derived by considering the Poisson equation with a simple counter-ion diffusion process. It has been also shown that the theoretical model with total co-ion exclusion provides an analytical solution for the steady-state electric potential at the ion exchange membrane-solution interface based on the Lambert W-function in the limit of low bathing ionic concentration with respect to the membrane fixed-charge concentration, which allows us to easily obtain the steady-state values of the surface electric charge, the ionic concentrations and the electric charge density at the interface.

ACKNOWLEDGMENTS

The author acknowledges the financial support from the Ministry of Economy and Competitiveness of Spain, Project FIS-47666-C3-2-R.

APPENDIX A

In this work, the study is presented by using dimensionless variables. They are obtained by dividing the variable by the following scaling factors:

- Molar concentration and fixed-charge concentration (mol m^{-3}): c_a

- Diffusion coefficient (m^2 s^{-1}): D_a

- Position and length (m): λ

- Time (s): $\frac{\lambda^2}{D_a}$

- Ionic flux (mol m^{-2} s^{-1}): $\frac{D_a c_a}{\lambda}$

- Electric potential (V): $\frac{RT}{F}$

- Electric field (V m^{-1}): $\frac{RT}{F\lambda}$

- Electric charge density (C m^{-3}): $F c_a$

- Electric displacement and surface electric charge (C m^{-2}): $F c_a \lambda$

- Electric permittivity (C V^{-1} m^{-1}): $\frac{F^2 c_a \lambda^2}{RT}$

- Electric current (A m^{-2}): $\frac{F D_a c_a}{\lambda}$

Here, the constants F, R and T have their usual meanings: Faraday constant (C mol^{-1}), ideal gas constant (J K^{-1} mol^{-1}) and absolute temperature (K), respectively. The parameters λ, D_a and c_a are scaling factors with the dimensions of length, diffusion coefficient and molar concentration, respectively. These three variables are chosen as characteristic values of the

system studied. In particular, the length λ is related to the Debye length in the system and it is chosen as:

$$\lambda = \sqrt{\frac{\varepsilon_M^* \varepsilon_0 R T}{F^2 c_a}}$$

where ε_M^* is the minimum value of the membrane relative dielectric constant and ε_0 the electric permittivity of the vacuum. The reader must note that the Debye length in a phase of a system is directly proportional to the square root of the electric permittivity of the medium. Since the dielectric constant of a membrane is similar or smaller than that of the solution, the Debye length in the membrane is the smallest length in the system and it is used as the scaling length. Using typical values of the diffusion coefficient and the ionic concentration in the solutions such 10^{-9} m^2/s and 0.05 M one obtains D_a=10^{-9} m^2/s and c_a=100 mM. Then, for ε_M^* =20, the normalization length of the system, λ, is approximately 3 nm. Thus, 1 unit of time, electric potential, surface electric charge, and capacitance is, respectively, 12 ns, 25 mV, 0.66 $\mu C/cm^2$, and 0.1 mF/cm^2.

APPENDIX B

The network simulation method[32] basically consists in modelling a physical or chemical process by means of a graphical representation analogous to circuit electrical diagrams, which is analysed by means of an electric circuit simulation program. Highly developed, commercially available software for circuit analysis (PSpice® from Cadence Design Systems) can thus be employed to obtain the dynamic behaviour of a system, without having to deal with the solution of the governing differential equations.[43] This method has previously demonstrated to be useful to study non-linear transport processes on the basis of the Nernst-Planck and Poisson equations in electrochemical cells and membrane systems and it is of a similar nature to those successfully used in other electrochemical systems dealing with mixed conductors[44-45] or complex kinetic schemes.[46]

The network model is obtained from a similar viewpoint to that of a finite difference scheme by dividing the physical region of interest, which we consider to have a unit cross-sectional area, into N volume elements or compartments of width δ_k (k=1, ..., N), small enough for the spatial variations of the parameters within each compartment to be negligible.[43] The network model for the diffusion-migration process of m ionic species in a compartment of width δ_k, which is extended from x_k-δ_k/2 to x_k+δ_k/2, is shown in Figure B1, and a complete explanation of the general procedure to obtain it can be found elsewhere.[28] In this figure, the network elements are as follows: R_{dik} is the resistor representing the diffusion of ion i in the compartment k; $GJ_{eik}(\pm)$ is the voltage-controlled current source modelling the electrical contribution to the ionic flux, minus and plus signs meaning the flux entering and leaving the compartment k, respectively; C_{dk} is the capacitor

representing the nonstationary effects of the electrodiffusion process in the compartment *k*; R_{Ck} is the resistor modelling the constitutive equation of the medium; and GJ_{Ck} is the voltage-controlled current source modelling the electric charge stores in the compartment *k*. The relation between those network elements and the parameters of the system is given by:

$$R_{dik} = \frac{\delta_k}{2D_{ip}} \tag{B1}$$

$$GJ_{eik}(\pm) = \pm D_{ip} z_i c_i (x_k \pm \frac{\delta_k}{2}) \frac{\phi(x_k) - \phi(x_k \pm \frac{\delta_k}{2})}{\delta_k / 2}, \qquad i = 1, \ldots, m \tag{B2}$$

$$C_{dk} = \delta_k \tag{B3}$$

$$R_{Ck} = \frac{\delta_k}{2\varepsilon_p} \tag{B4}$$

$$GJ_{Ck} = -\delta_k \rho_p (x_k) \tag{B5}$$

where D_{ip} and ε_p stand for the diffusion coefficients of ion *i* and the dielectric constant in the solution (*p*=*S*) and membrane (*p*=*M*) phases, respectively, while the electric charge density, ρ_p, must be evaluated from eq. 3 in the compartments belonging to the solution phase, $\rho_S(x_k)=z_1c_1(x_k)+z_2c_2(x_k)$, and from eq. 7 in those lying in the membrane phase, $\rho_M(x_k)=z_1c_1(x_k)-X$.

For network modelling purposes, a number *N* of network elements like those in Figure B1 (*k*=1,...,*N*) with the appropriate number of branches, values of the diffusion coefficients and the dielectric constant, and expressions of the electric charge density must be connected in series to form a network model for the entire physical region undergoing electrodiffusion processes.

Figure B2 shows the network model for the system constituted by the interfacial

region between a solution and an ion-exchange membrane with total co-ion exclusion. In this figure, the six-terminal box (S) is constituted by the series combination of N_1 elements such as that shown in Figure B1 with m=2 and the circuit elements corresponding to the solution phase, while the four-terminals one (M) is formed by the combination in series of N-N_1 elements such as that in Figure B1 with m=1 and the circuit elements corresponding to the membrane (M). In the network model of Figure B2, the concentrations of the ionic species in the bathing solution and in the bulk of the membrane, which are given by boundary conditions shown in eqs. 10a-c, are represented by independent voltage sources of values $c_{1L}=c^0$, $c_{2L}=-z_1c^0/z_2$, and $c_{1R}=X/z_1$. In this network, the branches modelling the counter-ion flux and the electric displacement in the solution and membrane phases are joined at the interface according to the boundary conditions given by eq. 11a and 13, respectively, while the branch modeling the co-ion flux in the solution must be open-circuited at the interface, because the membrane presents total co-ion exclusion according to eq. 11b. On the other hand, the equilibrium state of the system is introduced in the network of Fig. B2 from a controlled current source, G_I, which takes the value of the electric displacement obtained from integration of the faradaic current with minus sign at the bathing solution such as given by eq. 12a, while the reference level for the electric potential given by eq. 12b is incorporated by short-circuiting the branch modelling the electric displacement at the bulk of the membrane. Finally, the initial conditions for the ionic concentrations and the electric potential are introduced as the initial voltages at the appropriate nodes of the network with the values given by eqs. 14a-d.

The spatial grid (N and δ_k) chosen considers the presence of the membrane-solution interface and both the solution and membrane phases. This spatial grid is symmetrical about

the solution-membrane interface (N_I=N/2). In the solution phase we have chosen 900 compartments uniformly distributed from x=-L to x=-10, 600 compartments from x=-10 to x=-4, 600 compartments from x=-4 to x=-1, and 400 compartments from x=-1 to x=0. In this way, N=5000 compartments have been used: 2500 for each phase.

Simulation of the network model shown in Figure B2 with the appropriate values for the parameters of the system into the PSpice® program under transient conditions, allows us to study the process of the formation of the electric double layer at the interface between an ion-exchange membrane and a solution, whatever the parameters of the system and the experimental conditions may be.

REFERENCES

1 J.W. Perram and P.J. Stiles, *Phys. Chem. Chem. Phys.*, 2006, **8**, 4200-4213.

2 E.J.F. Dickinson, L. Freitag and R.G. Compton, *J. Phys. Chem. B*, 2010, **114**, 187-197.

3 K.R. Ward, E.J.F. Dickinson and R.G. Compton, *J. Phys. Chem. B*, 2010, **114**, 4521-4528.

4 D. Britz and J. Strutwolf, *Electrochim. Acta*, 2014, **137**, 328-335.

5 K.R. Ward, E.J.F. Dickinson and R.G. Compton, *J. Phys. Chem. B*, 2010, **114**, 10763-10773.

6 K.R. Ward, E.J.F. Dickinson and R.G. Compton, *Int. J. Electrochem. Sci.*, 2010, **5**, 1527-1534.

7 H. Strathmann, *Desalination*, 2010, **264**, 268-288.

8 J.M. Zook, R.P. Buck, J. Langmaier and E. Lindner, *J. Phys. Chem. B*, 2008, **112**, 2008-2015.

9 B.E. Logan and M. Elimelech, *Nature*, 2012, **488**, 313-319.

10 G. Merle, M. Wessling and K. Nijmeijer, *J. Membr. Sci.*, 2011, **377**, 1-35.

11 W. Wang, Q. Luo, B. Li, X. Wei, L. Li and Z. Yang, *Adv. Funct. Mater.*, 2013, **23**, 970-986.

12 R.A. Rica, R. Ziano, D. Salerno, F. Mantegazza, M.A. Bazant, M.A. and D. Broglioli, *Electrochim. Acta*, 2013, **92,** 304-314.

13 S. Porada, R. Zhao, A. van der Wal, V. Presser and P.M. Biesheuvel, *Prog. Mater. Sci.*, 2013, **58**, 1388-1442.

14 H. Miyoshi, *J. Membr. Sci.*, 1998, **141**, 101-110.

15 C. Larchet, L. Dammak, B. Auclair, S. Parchikov and V. Nikonenko, *New J. Chem.*, 2004, **28**, 1260-1267.

16 H. Zhu, H. Ghoufi, A. Szymczyk, B. Balannec and D. Morineau, *Phys. Rev. Lett.*, 2012, **109**, 107801:1-5.

17 G. Barbero and I. Lelidis, *J. Appl. Phys.*, 2014, **115**, 194101:1-4.

18 K. Konturri, L. Murtomäki and J.A. Manzanares, *Ionic transport processes in electrochemistry and membrane science*, Oxford University Press, NY, 2008.

19 P. Magnico, *J. Membr. Sci.*, 2013, **442**, 272-282.

20 Y. Lanteri, A. Szymczyk and P. Fievet, *Langmuir*, 2008, **24**, 7955-7962.

21 Y. Lanteri, A. Szymczyk and P. Fievet, *J. Phys. Chem. B*, 2009, **113**, 9197-9204.

22 A. Escoda, Y. Lanteri, P. Fievet, S. Déon and A. Szymczyk, *Langmuir*, 2010, **26**, 14628–14635.

23 V. Shapiro, V. Freger, C. Linder, Y. Oren, *J. Phy. Chem. B*, 2008, **112**, 9389–9399.

24 W. Kucza, M. Danielewski and A. Lewenstam, *Electrochem. Commun.*, 2006, **8**, 416-420.

25 B. Grysakowski, J.J. Jasielec, B. Wierzba, T. Solkalski, A. Lewentam and M. Danielewski, *J. Electroanal. Chem.*, 2011, **662**, 143-149.

26 T.R. Brumleve and R.P. Buck, *J. Eleactroanal. Chem.*, 1978, **90**, 1-31.

27 J.A. Manzanares, W.D. Murphy, S. Mafé and H. Reiss, *J. Phys. Chem.*, 1993, **97**, 8524-8530.

28 A.A. Moya and J. Horno, *J. Phys. Chem. B*, 1999, **103**, 10791-10799.

29 T. Sokalski, P. Lingenfelter and A. Lewenstam, *J. Phys. Chem. B*, 2003, ***107***, 2443-

2452.

30 V.M. Volgin and A.D. Davydov, *J. Membr. Sci.*, 2005, **259**, 110-121.

31 W.E. Morf, E. Pretsch and N.F. De Rooij, *J. Electroanal. Chem.*, 2007, **602**, 43-54.

32 A.A. Moya, *J. Phys. Chem. C*, 2014, **118**, 2539-2553.

33 G. Pourcelly, P. Sistat, A. Chapotot, C. Gavach and V. Nikonenko, *J. Membr. Sci.*, 1996, **110**, 69-78.

34 F. Ciucci, W.C. Chueh, D.G. Goodwin and S.M. Haile, *Phys. Chem. Chem. Phys.*, 2011, **13**, 2121–2135.

35 C. Chen, D. Chen, W.C. Chueh and F. Ciucci, *Phys. Chem. Chem. Phys.*, 2014, **16**, 11573-11583.

36 A.J. Bard and L.R. Faulkner, *Electrochemical Methods: Fundamentals and Applications*, Wiley, NY, 2001.

37 A.A. Moya, *Electrochim. Acta*, 2011, **56**, 3015-3022.

38 A.A. Moya, *Electrochim. Acta*, 2012, **62**, 296-304.

39 A.A. Moya, *Electrochim. Acta*, 2013, **90**, 1-11.

40 J.A. Manzanares, S. Mafé and J. Bisquert, *Ber. Bunsenges. Phys. Chem.*, 1992, **96**, 538-544.

41 http://functions.wolfram.com/ElementaryFunctions/ProductLog/07/ShowAll.html

42 A.H. Galama, J.W. Post, M.A. Cohen Stuart and P.M. Biesheuvel, J. Membr. Sci., 2013, **442**, 131-139.

43 J. O'M. Bockris and A.K.N. Reddy, *Modern Electrochemistry*, Plenum Press, NY and London, 1998.

44 J. Jamnik and J. Maier, *Phys. Chem. Chem. Phys.*, 2001, **3**, 1668-1678.

45 F. Ciucci and W. Lai, *Electrochim. Acta*, 2012, **81**, 205-215.

46 M. Caravaca, P. Sánchez-Andrada, A. Soto and M. Alajarín, *Phys. Chem. Chem. Phys.*, 2014, **16**, 25409-25420.

Tables

Table 1. Numerical results for ϕ_{SS}, ϕ_R and σ, in systems with z_1=1, z_2=-1, ε_S=4, X=5, and different values of ε_M, and c^0.

		ε_M=4		ε_M=2		ε_M=1	
c^0	ϕ_{SS}	ϕ_R	σ	ϕ_R	σ	ϕ_R	σ
0.01	6.215	1.000	3.850	1.284	3.350	1.612	2.848
0.05	4.605	0.9809	3.773	1.249	3.273	1.556	2.770
0.1	3.912	0.9611	3.707	1.219	3.207	1.510	2.729
0.5	2.303	0.8228	3.237	1.017	2.752	1.221	2.271
1	1.609	0.6789	2.728	0.8216	2.286	0.9638	1.858
2	0.9163	0.4512	1.877	0.5322	1.546	0.6086	1.236
4	0.2231	0.1258	0.5510	0.1444	0.4458	0.1611	0.3509

Figure Captions

Fig. 1. Time evolution of the interfacial electric in a system with z_1=1, z_2=-1, L=20, ε_S=4, D_{1S}=1, D_{2S}=1.5, X=5, ε_M=4, c^0=0.5, and different values of D_{1M}, namely, D_{1M}=1, 0.1, and 0.01. The arrow indicates decreasing values of D_{1M}.

Fig. 2. Time evolution of the surface electric charge in the solution diffuse layer under the same conditions given in Fig. 1.

Fig. 3. Time evolution of the interfacial potential in systems with z_1=1, z_2=-1, L=20, ε_S=4, D_{1S}=1, D_{2S}=1.5, D_{1M}=0.1, X=5, ε_M=4, c^0=0.5, and different values of ε_M, namely, ε_M=4, 2, and 1. The arrow indicates decreasing values of ε_M.

Fig. 4. Time evolution of the surface electric charge in the solution diffuse layer under the same conditions given in Fig. 3.

Fig. 5. Evolution of the steady-state values of the interfacial potential, ϕ_{SS}, and the electric potential difference at the membrane diffuse double layer, ϕ_R, with the bathing electrolyte concentration, c^0, in systems with z_1=1, z_2=-1, L=20, ε_S=4, D_{1S}=1, D_{2S}=1.5, D_{1M}=0.1, X=5, and different values of ε_M, namely, ε_M=4, 2, and 1. The arrow indicates decreasing values of ε_M.

Fig. 6. Evolution of the steady-state value of the surface charge density, σ_{SS}, with the bathing electrolyte concentration, c^0, under the same conditions given in Fig. 5.

Fig. 7. Profiles of the cationic concentration at the interfacial region of a system with z_1=1, z_2=-1, L=20, ε_S=4, D_{1S}=1, D_{2S}=1.5, D_{1M}=0.1, X=5, and ε_M=2, for different times.

Fig. 8. Profiles of the anionic concentration under the same conditions given in Fig. 7.

Fig. 9. Profiles of the electric charge density under the same conditions given in Fig. 7.

Fig. 10. Profiles of the electric displacement under the same conditions given in Fig. 7.

Fig. 11. Profiles of the electric potential under the same conditions given in Fig. 7.

Fig. B1. Network model for the electrodiffusion of m ionic species in a volume element.

Fig. B2. Network model for the interfacial region between ion-exchange membrane and solution. The six and four-terminals boxes are obtained by the combination in series of structures such as those shown in Fig. B1.

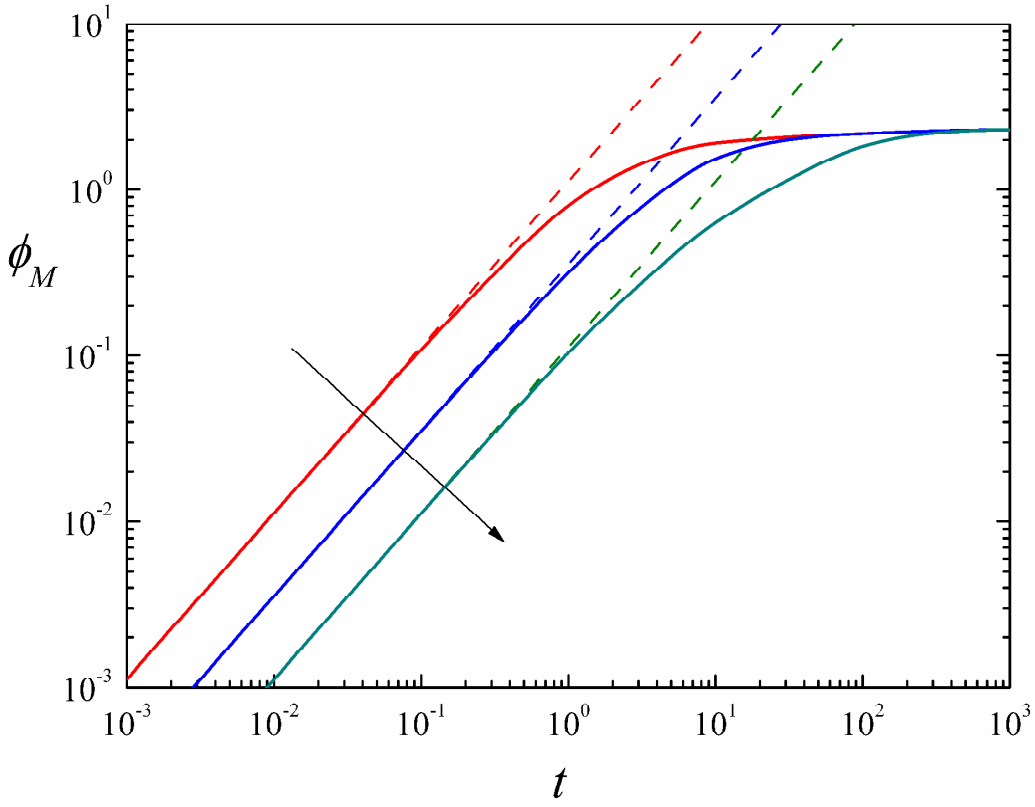

Fig. 1

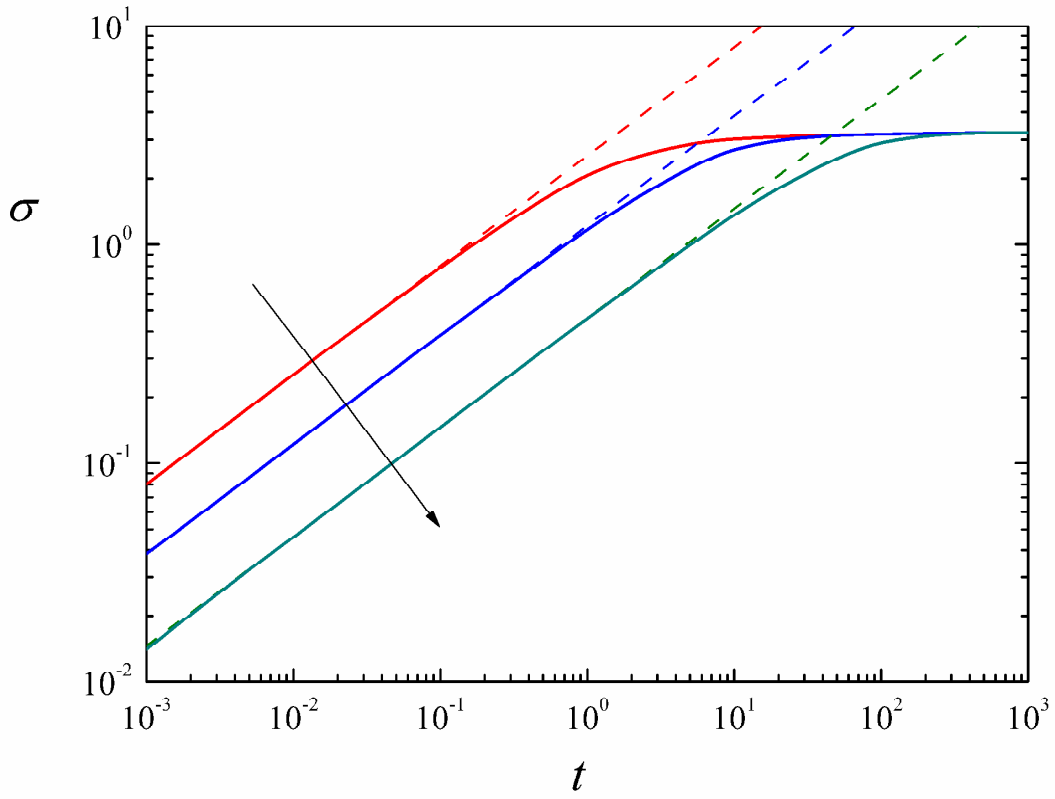

Fig. 2

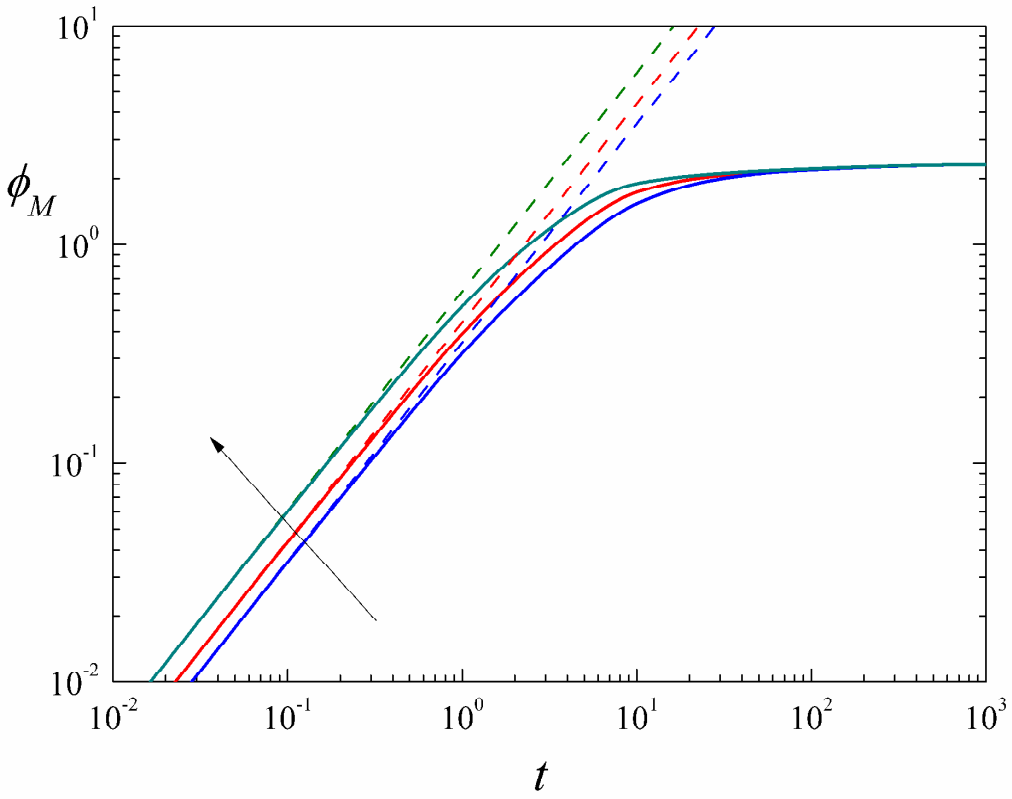

Fig. 3

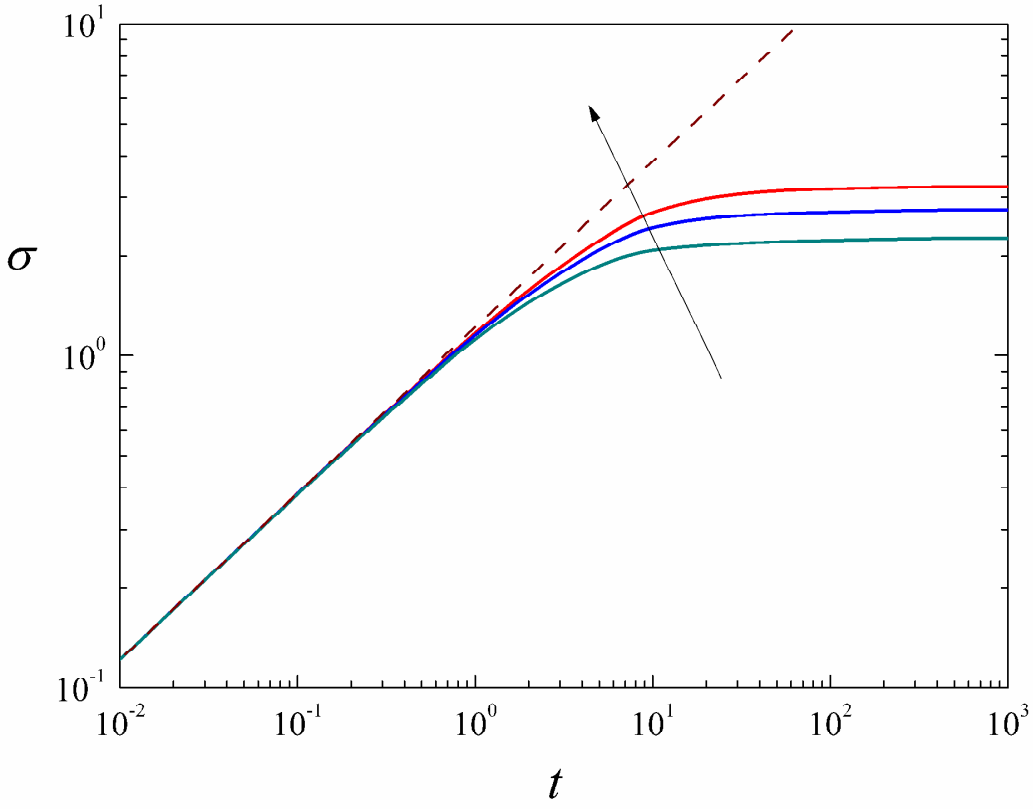

Fig. 4

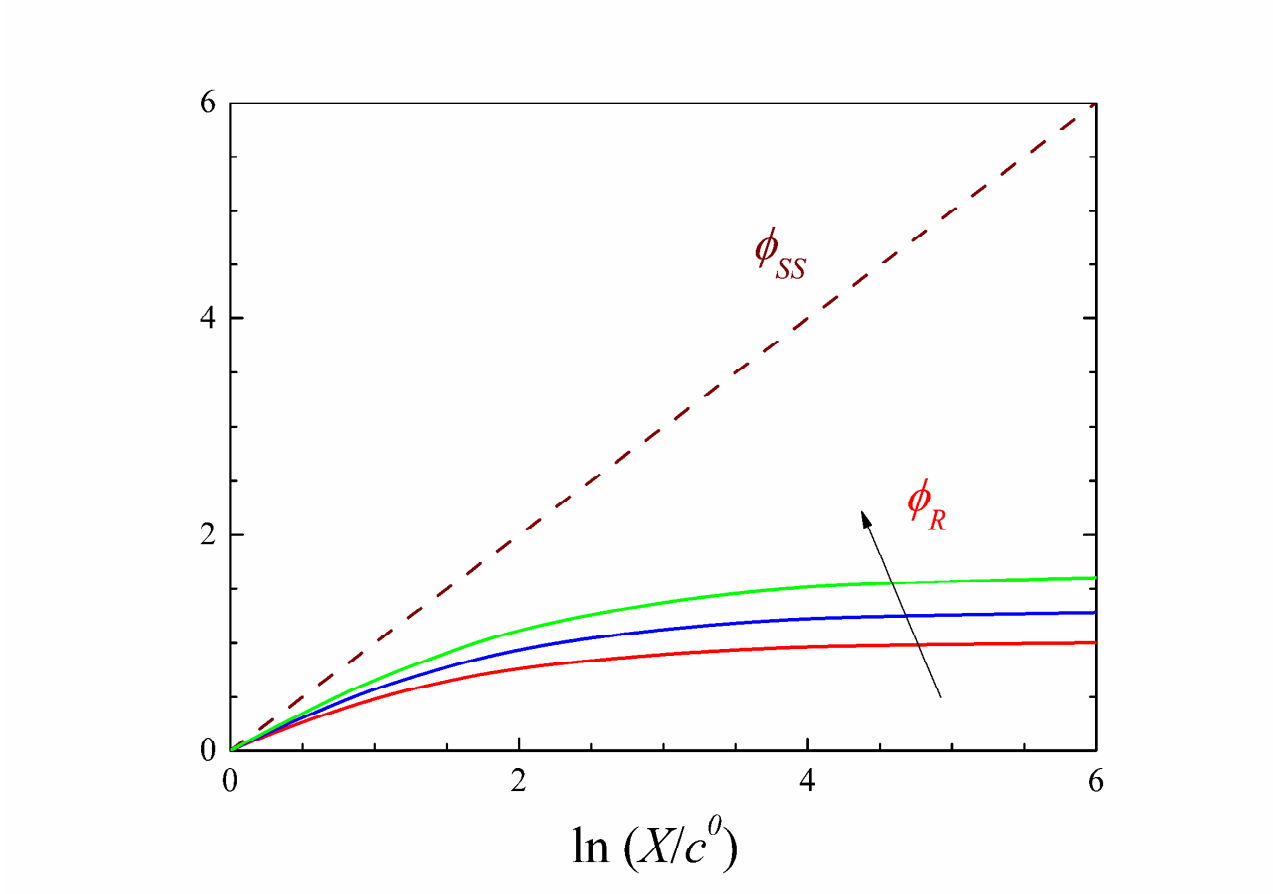

Fig. 5

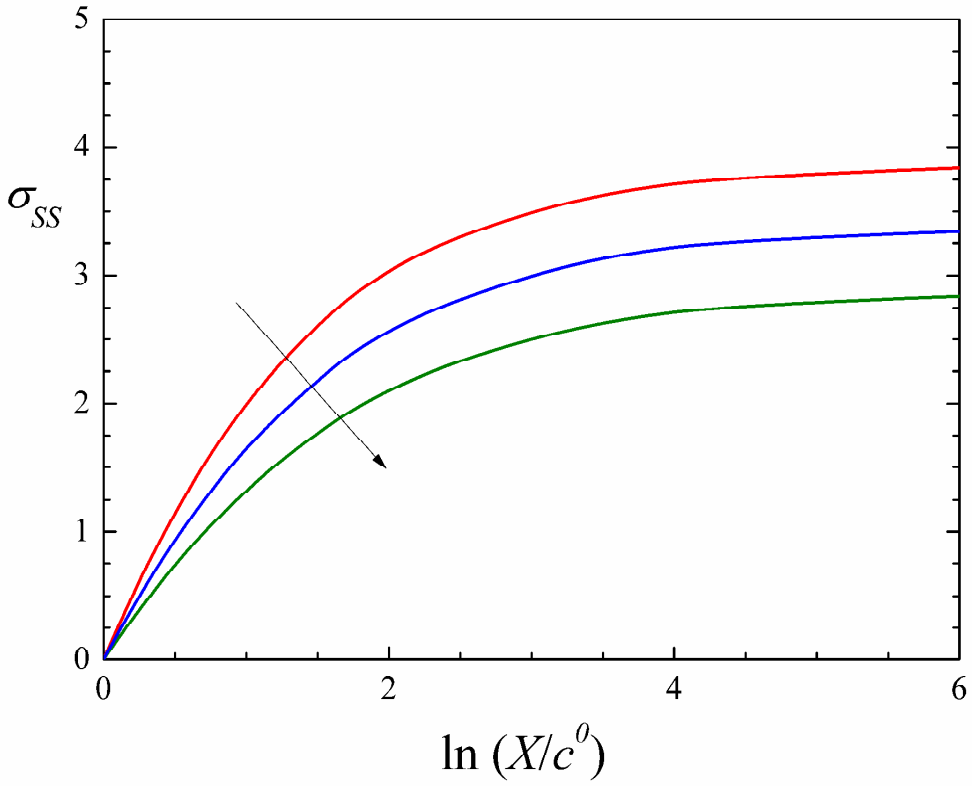

Fig. 6

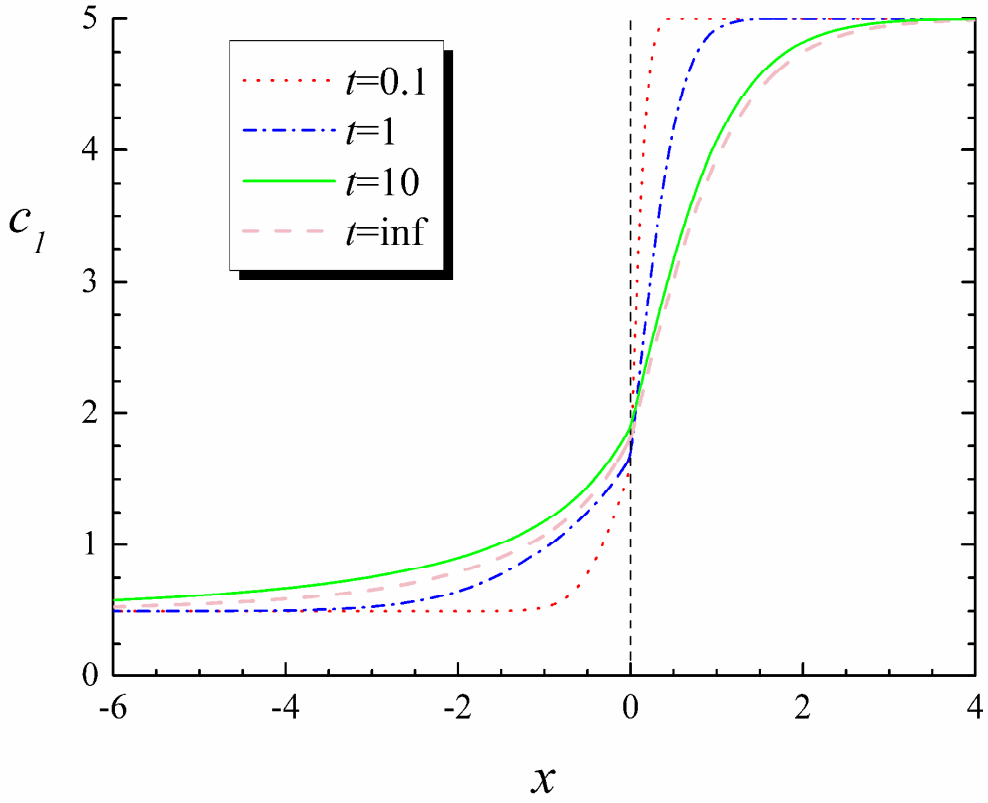

Fig. 7

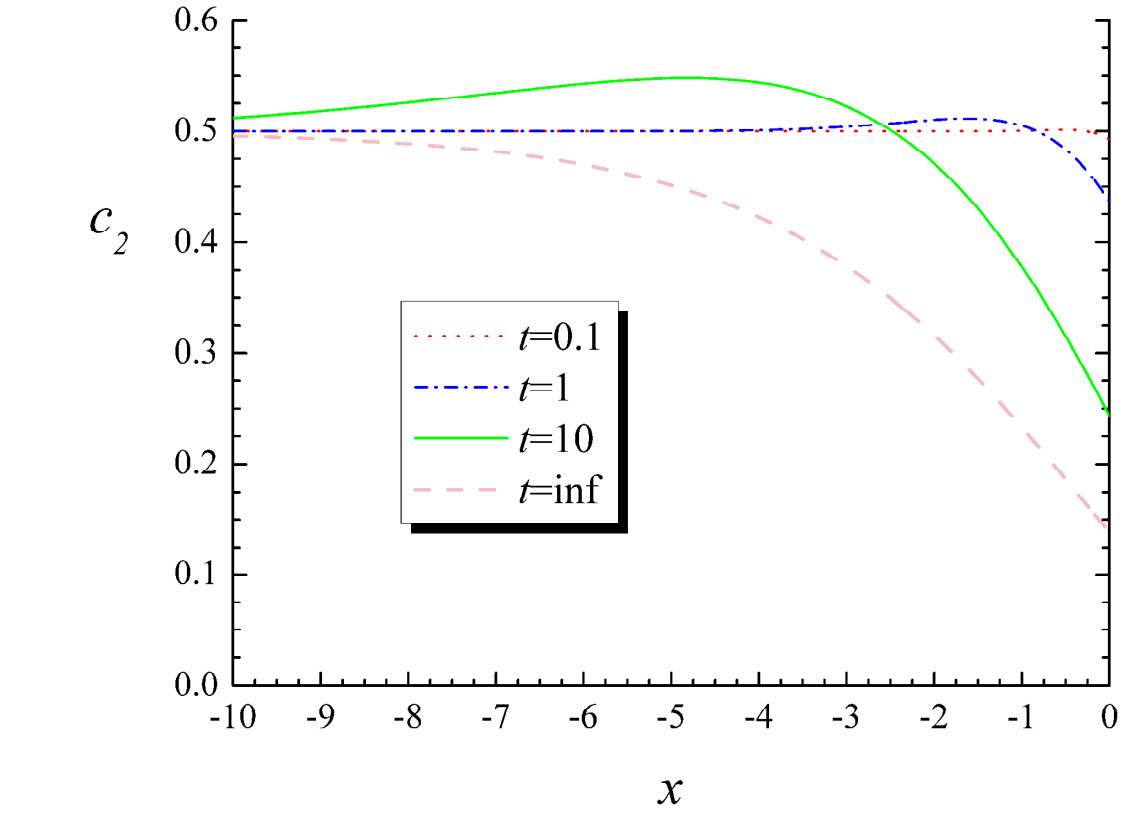

Fig. 8

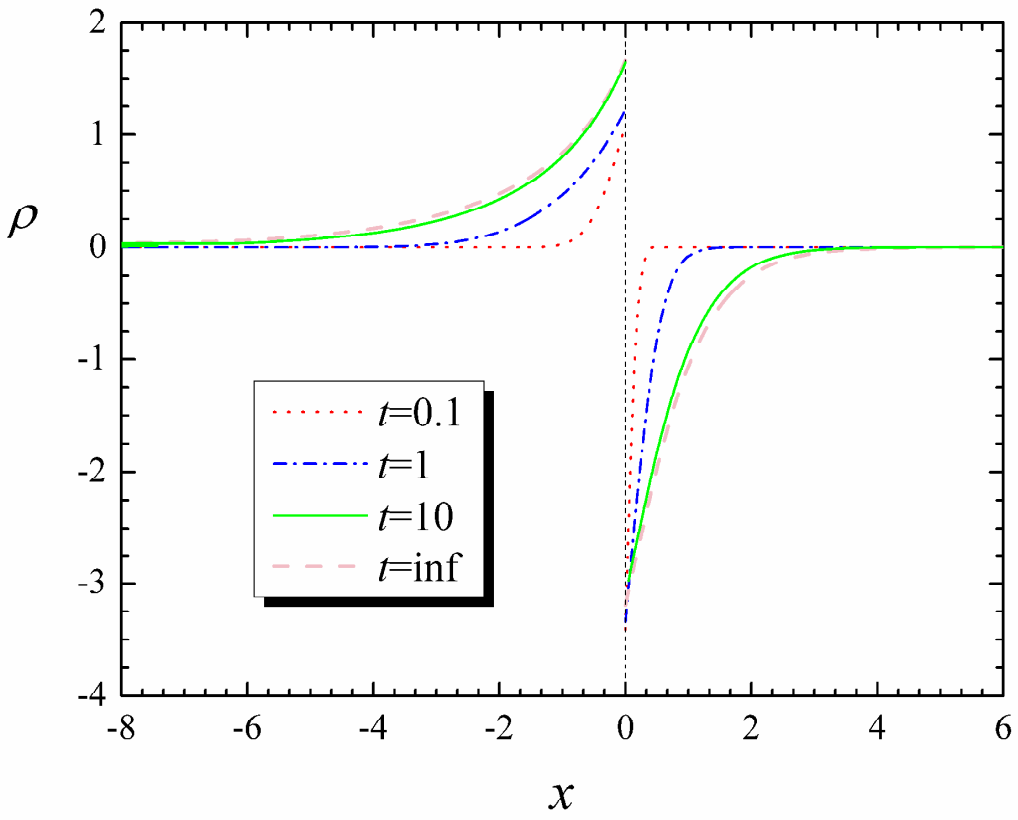

Fig. 9

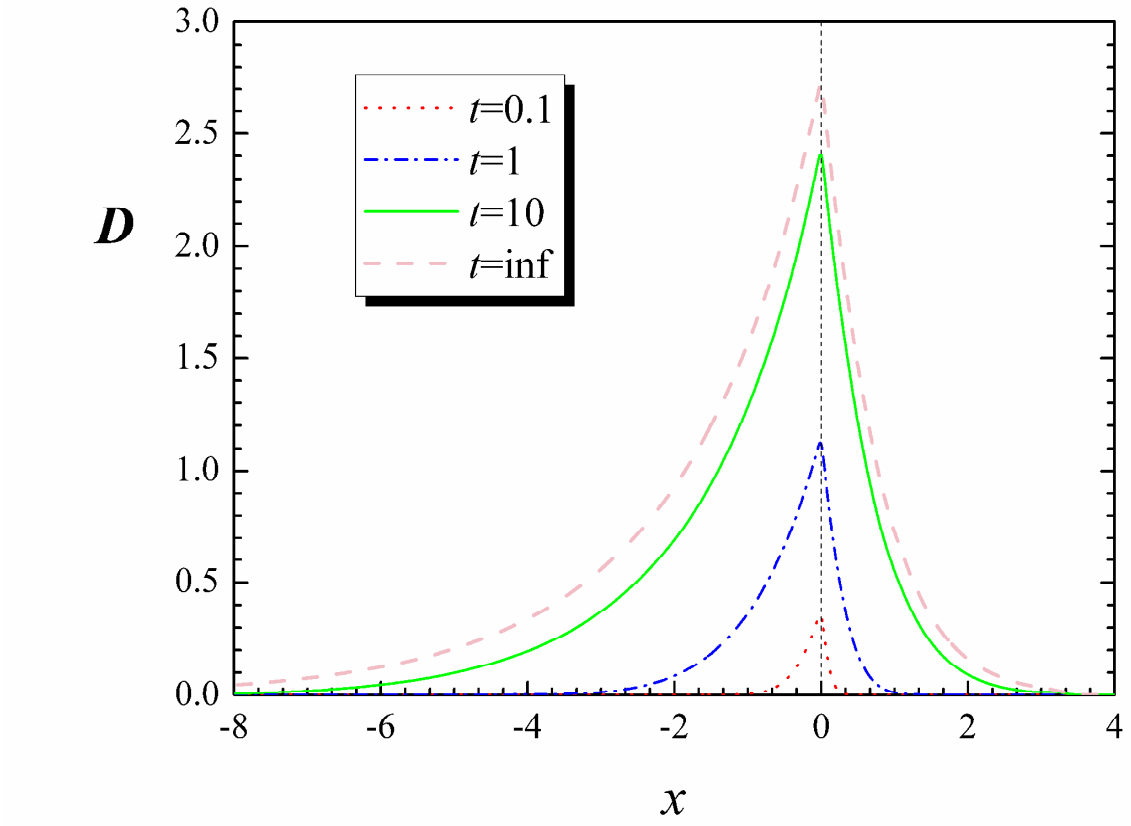

Fig. 10

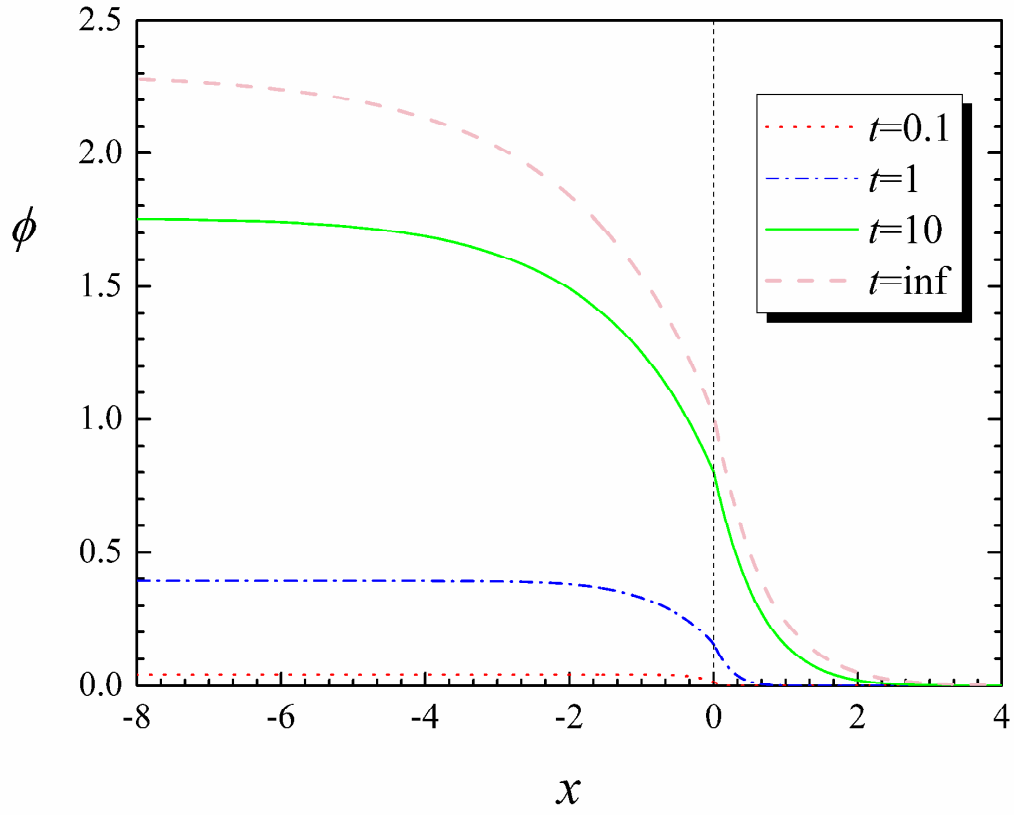

Fig. 11

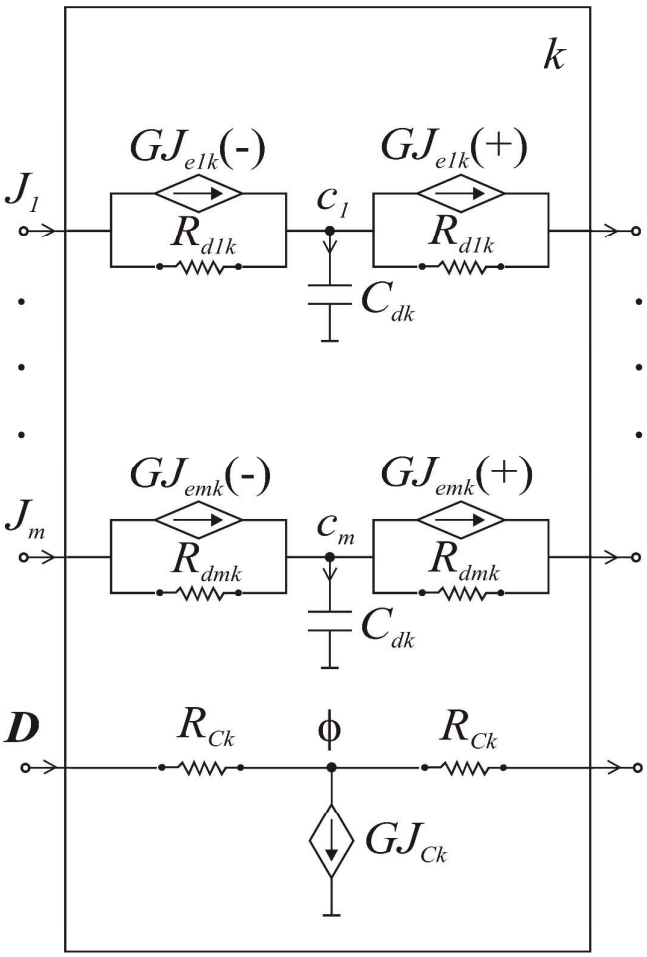

Fig. B1

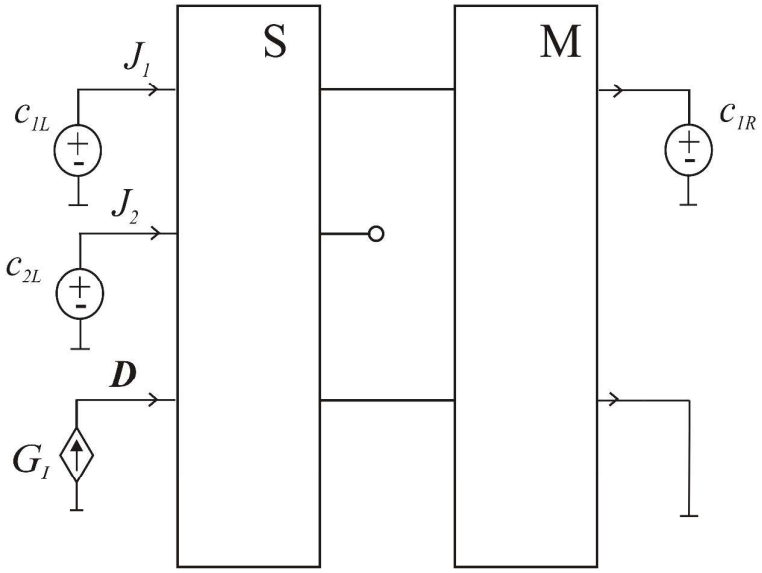

Fig. B2